JACS
JOURNAL OF THE AMERICAN CHEMICAL SOCIETY
pubs.acs.org/JACS
Article

In Situ Generated CO Enables High-Current CO_2 Reduction to Methanol in a Molecular Catalyst Layer

Seonjeong Cheon, Jing Li, and Hailiang Wang*

Cite This: *J. Am. Chem. Soc.* 2024, 146, 16348−16354
Read Online
ACCESS | Metrics & More | Article Recommendations | Supporting Information

ABSTRACT: Molecular catalysts such as cobalt phthalocyanine (CoPc) exhibit remarkable electrochemical activity in methanol production from CO_2 or CO, but fast conversion with a high current density is still yet to be realized. While adopting flow cells with gas diffusion electrodes is a common approach to enhanced reaction rates, the current scientific and engineering knowledge primarily centers on metal particle-based catalysts like Cu. This focus overlooks the emerging heterogenized molecular catalysts with distinct physical and chemical properties. In this work, we observe that the partial current density of CO reduction to methanol catalyzed by tetraamine-substituted CoPc (CoPc-NH_2) supported on carbon nanotubes (CNTs) remains below 30 mA cm^{-2}, even with systematic optimization of structural and operational parameters of the flow cell. A comparative analysis with a Cu metal catalyst reveals that the porous and electrolyte-philic nature of CoPc-NH_2/CNT leaves a large fraction of active sites deprived of CO under reaction conditions. To address this microenvironmental challenge, we directly use CO_2 as the reactant, leveraging its faster diffusion rate in water compared to CO. Effective CO_2 reduction generates CO *in situ* to feed the catalytic sites, achieving an unprecedently high partial current density for methanol of 129 mA cm^{-2}. This research underscores the necessity for new insights and approaches in the development of molecular catalyst-based electrodes.

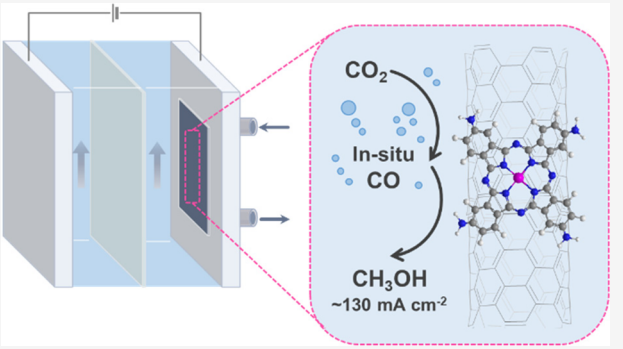

INTRODUCTION

Electrochemical CO_2 reduction is an effective way to recycle carbon emissions into valuable chemicals and store renewable electricity.[1−4] Among a variety of products, methanol is particularly attractive as a clean liquid fuel and a base material for thousands of commercial products.[5,6] However, the pool of known electrocatalysts proficient in converting CO_2 to methanol remains limited.[7−9] One promising strategy is to use molecular catalysts whose single-atom active sites have the advantage of suppressing C_{2+} products. Their well-defined molecular structures also allow for precise tailoring of the catalytic sites.[10,11] We previously reported that cobalt phthalocyanine molecules supported on multiwalled carbon nanotubes (CoPc/CNT) can produce methanol from CO_2 electroreduction with an appreciable yield.[12] The catalytic activity appears to originate from the intrinsic structure of CoPc, with the performance notably enhanced by the high-level dispersion of the molecules and the facile electron transfer from the highly conductive CNT support.[13,14] Importantly, the CO_2-to-methanol conversion on CoPc/CNT involves CO as a key intermediate, and a high local concentration of CO is needed to promote methanol production.[12,15] Thus, investigating CO reduction is critical for advancing the catalytic performance of the molecular catalyst toward practical application.

Our original CoPc/CNT catalyst showed a 28% Faradaic efficiency (FE_{MeOH}) with a 3 mA cm^{-2} partial current density (j_{MeOH}) for methanol production from CO reduction, whereas the tetraamine-substituted catalyst version (CoPc-NH_2/CNT) exhibited a higher FE_{MeOH} of 41% with a better stability.[12] With a microporous layer to enhance CO mass transport, CoPc-NH_2/CNT showed a 66% FE_{MeOH} with a 7.8 mA cm^{-2} j_{MeOH} in an H-cell.[15] However, the reaction rate was still constrained by the low solubility of CO in water (~1 mM at 25 °C). To overcome this mass transport limitation, recent studies have adopted flow cells with gas diffusion electrodes (GDEs) to enhance current density.[16,17] GDEs, designed with hydrophobic channels to facilitate the delivery of gaseous reactants to catalysts through a relatively thin layer of electrolyte,[16,18] significantly greatly reduce the diffusion layer thickness from ~50 μm in an H-cell to ~50 nm.[19] Leveraging GDE-based cell designs, various CoPc-based catalysts have achieved peak j_{MeOH} in the range of 19.5 to 62.1 mA

Received: May 1, 2024
Revised: May 21, 2024
Accepted: May 21, 2024
Published: May 28, 2024

https://doi.org/10.1021/jacs.4c05961
J. Am. Chem. Soc. 2024, 146, 16348−16354

cm^{-2}.[20−23] Despite the considerable progress over H-cell performance, the reaction rate (i.e., current density) still lags behind the state-of-the-art for CO_2 electrolyzers by 1 order of magnitude.[24−27]

In this work, we first explored CO reduction catalyzed by CoPc-NH_2/CNT in a flow cell. Following a systematic optimization of various parameters on the catalyst, electrode, and reactor levels, we achieved FE_{MeOH} up to 60%, but j_{MeOH} remained below 30 mA cm^{-2}. Through control experiments and comparison with a Cu metal catalyst, we found that the slow CO-to-methanol conversion rate is related to the porous structure of the CoPc-NH_2/CNT catalyst layer and its electrolyte-philic surfaces (Figure 1c). In this scenario,

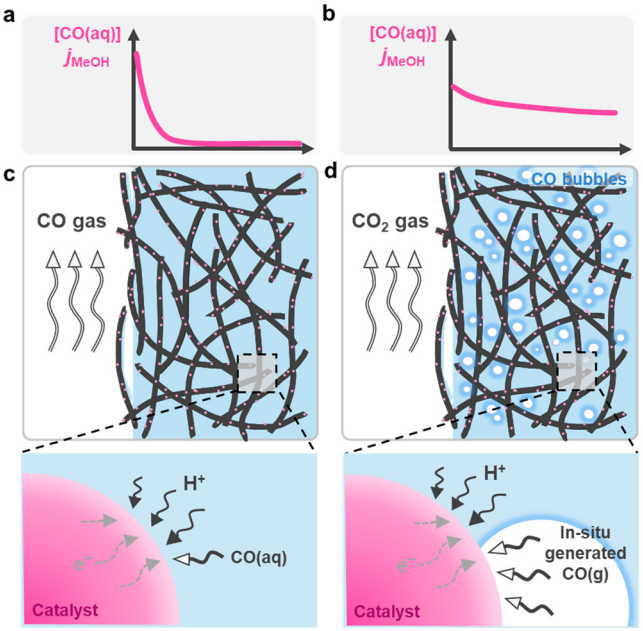

Figure 1. CO vs CO_2 reduction in CoPc-NH_2/CNT catalyst layer. CO concentration profile and methanol partial current density profile along the electrolyte-occupied catalyst layer in (a) CO vs (b) CO_2 reduction. Microenvironment of the electrolyte-occupied catalyst layer (c) relying on dissolved CO for the methanol generation reaction in CO reduction vs (d) utilizing *in situ* generated CO for methanol production in CO_2 reduction.

although gaseous CO is supplied through the gas diffusion layer, a large portion of catalytic sites remain deprived of CO due to its low water solubility (Figure 1a). We resolved this problem by directly using CO_2 as the reactant, leveraging its faster diffusion rate than CO in the electrolyte owing to its 30 times higher water solubility. Effective CO_2 reduction generates abundant CO within the catalyst layer to support high-rate reduction into methanol (Figure 1d). Ultimately, CO_2 reduction, compared to CO reduction, enables the use of a much thicker CoPc-NH_2/CNT catalyst layer and achieves more than four times faster methanol production (Figure 1b).

RESULTS AND DISCUSSION

CO Reduction Performance. The CO reduction catalyzed by CoPc-NH_2/CNT (Figures S1−S3) was conducted in a three-compartment flow cell with eight important structural and operational parameters taken into consideration (Figure 2a). As the flow cell is designed to provide sufficient reactants to the catalytic sites, the number of cobalt sites is anticipated to influence CO reduction performance. Hence, we first varied the mass ratio of CoPc-NH_2 to CNT in the catalyst material (Figure S4). Tested with all the other parameters held constant (Table S1), the electrodes exhibited noticeable changes in FE_{MeOH} and j_{MeOH} as the mass ratio of CoPc-NH_2 to CNT was increased from 5 to 25 wt % (Figure 2b). The highest FE_{MeOH} (62.4%) was obtained with 20 wt % of CoPc-NH_2, while the largest j_{MeOH} (18.7 mA cm^{-2}) was achieved at 15 wt %. This observation may be attributed to the possible aggregation of CoPc-NH_2 molecules on CNT surfaces at CoPc-NH_2 loadings exceeding 15 wt % (Figure S5). We then varied the catalyst mass loading from 0.2 to 1.6 mg cm^{-2}. Best FE_{MeOH} and j_{MeOH} were both attained at 0.4 mg cm^{-2} (Figure 2c), suggesting that most of the additional catalytic sites beyond this mass loading are not effectively used to catalyze CO reduction. Further discussion on this phenomenon will be provided in the text below.

Our prior work demonstrated that $KHCO_3$ is a desirable proton donor for methanol production from CO reduction on CoPc-NH_2/CNT.[15] Therefore, we examined $KHCO_3$ electrolyte solutions with varying concentrations. As the concentration was increased from 0.1 to 0.3 M, j_{MeOH} rose from 12.3 to 25.1 mA cm^{-2}, while the selectivity for methanol exhibited no significant change (Figure 2d). It suggests that $KHCO_3$ is an effective proton donor for both methanol formation and H_2 evolution within this concentration range. However, with further concentration increase, FE_{MeOH} declined and j_{MeOH} remained constant, which is consistent with our understanding that higher $KHCO_3$ concentrations favor H_2 evolution over CO reduction.[15] Another approach to influence proton transfer involves adjusting the amount of ionomer, which can also modify local concentrations of ions, water, and gaseous reactants through its hydrated hydrophilic groups and hydrophobic backbone.[28,29] In our experiments, the highest methanol selectivity and production rate were achieved with a Nafion-to-catalyst ratio of 66 wt % (Figure 2e). Flow cell operational parameters such as CO and electrolyte flow rates did not affect the performance notably within the studied ranges (Figure 2f, g).

Based on the optimized conditions, we investigated the potential dependency. Consistent with our prior work obtained in an H-cell,[15] a maximum FE_{MeOH} of 44% was realized at −0.8 V_{RHE}, and the selectivity decreased as the potential became more negative due to enhanced H_2 evolution (Figure 2h). The highest j_{MeOH}, 13.7 mA cm^{-2}, appeared at −0.9 V_{RHE}. Additionally, we operated the cell in the constant current mode. FE_{MeOH} continuously decreased as the current was increased from 25 to 200 mA cm^{-2} (Figure 2i). The highest j_{MeOH}, 22 mA cm^{-2}, was achieved at 100 mA cm^{-2}. It is noteworthy that although employing GDEs with flow cells has been shown to be effective in increasing the reduction rate of CO, which has inherently low water solubility, on commonly used metal particle-based catalysts, the same approach is not directly applicable to heterogeneous molecular catalysts like CoPc-NH_2/CNT.

Comparison between CoPc-NH_2/CNT and Cu. It was surprising that, despite our systematic optimization, the methanol production performance of CoPc-NH_2/CNT from CO reduction in the flow cell, especially the partial current density, remained below 30 mA cm^{-2}, only twice the highest value observed in our H-cell.[15] This raised suspicions about the correct configuration of our flow cell and the capability of our CoPc-NH_2/CNT catalyst to deliver a high reaction rate. To

https://doi.org/10.1021/jacs.4c05961
J. Am. Chem. Soc. 2024, 146, 16348−16354

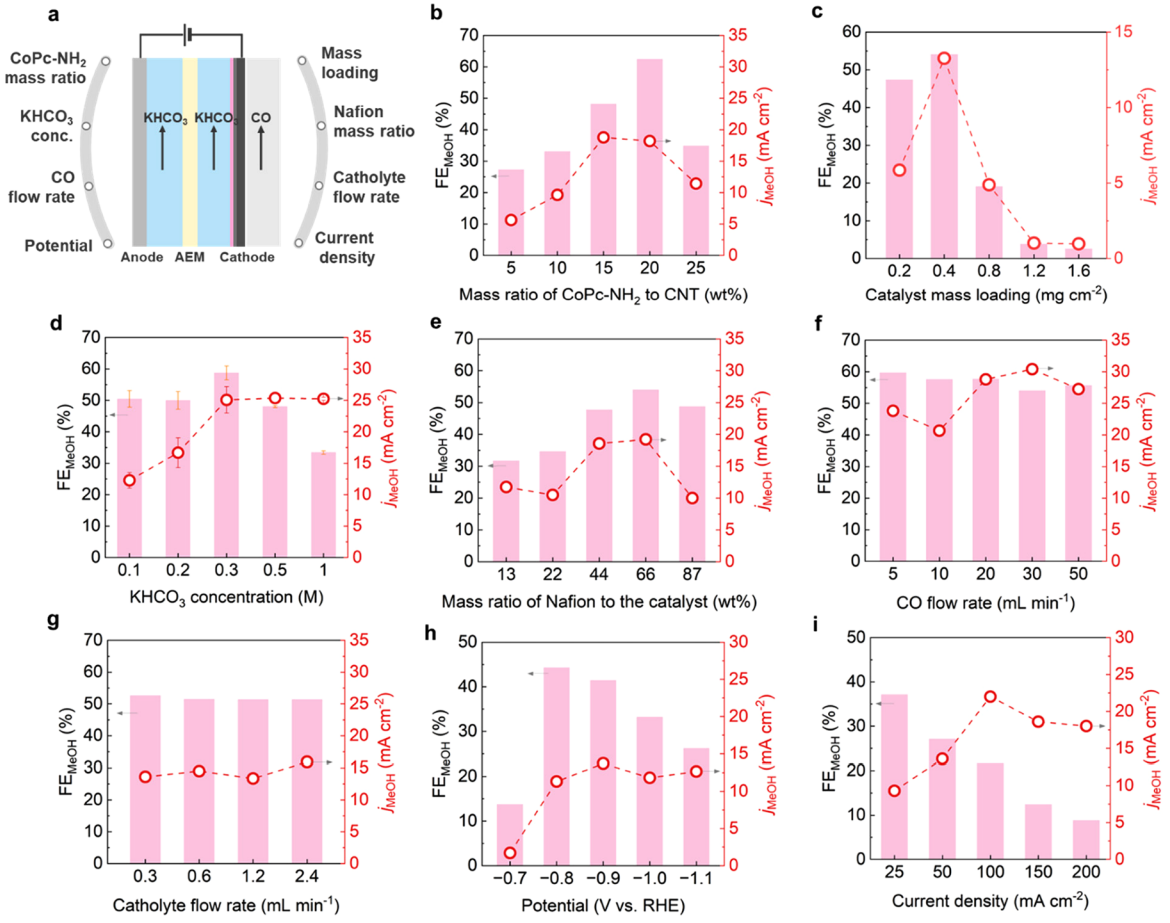

Figure 2. CO reduction performance catalyzed by CoPc-NH_2/CNT in flow cell. (a) Investigated parameters for optimizing performance. Faradaic efficiency and partial current density of methanol vs (b) mass ratio of CoPc-NH_2 to CNT, (c) mass loading of catalyst, (d) $KHCO_3$ concentration, (e) mass ratio of Nafion to the catalyst, (f) CO flow rate, (g) catholyte flow rate, (h) applied potential, and (i) applied total current density. See Table S1 for detailed experimental conditions.

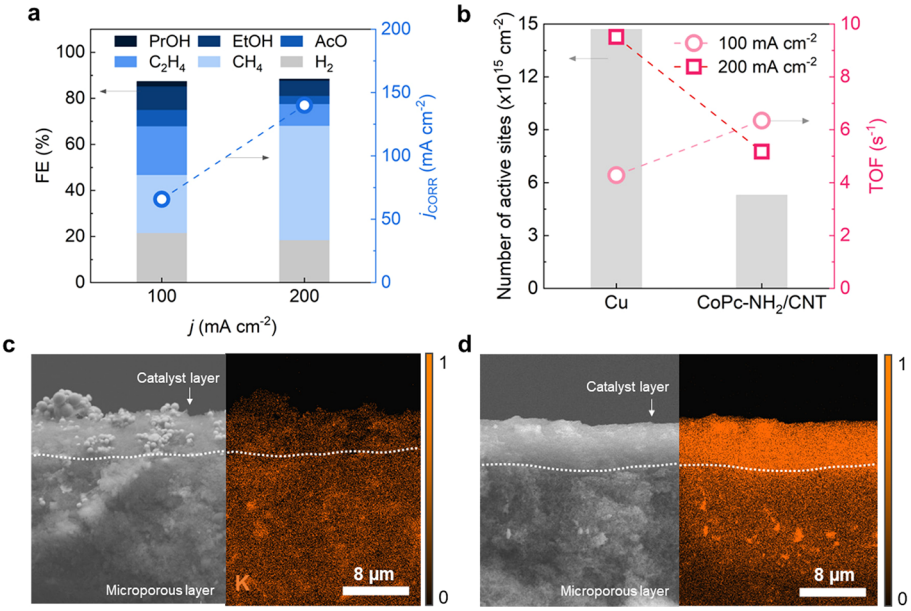

Figure 3. Comparison of CO reduction rate between Cu microparticle and CoPc-NH_2/CNT catalysts. (a) CO reduction performance of Cu in 0.2 M $KHCO_3$. (b) Comparison of the number of electrochemically active sites and TOF between Cu and CoPc-NH_2/CNT under constant current conditions. Cross-sectional SEM images (left) and corresponding K EDS maps (right) of (c) Cu and (d) CoPc-NH_2/CNT electrodes after CO reduction at 50 mA cm^{-2}. See Table S2 for detailed experimental conditions.

https://doi.org/10.1021/jacs.4c05961
J. Am. Chem. Soc. 2024, 146, 16348−16354

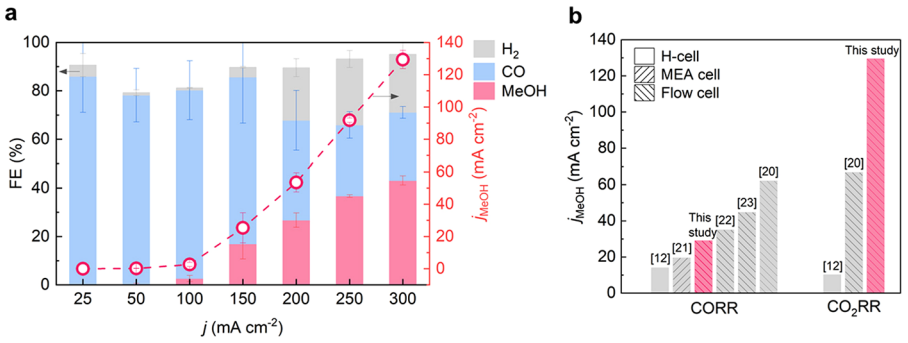

Figure 4. CO_2 reduction performance catalyzed by CoPc-NH_2/CNT. (a) Faradaic efficiency and partial current density of methanol from CO_2 reduction in the flow cell at different total current densities in 0.3 M $KHCO_3$. (b) Performance comparison of methanol production from CO_2 and CO reduction using CoPc-based catalysts. See Tables S4 and S5 for details.

figure out the underlying reason, we replaced CoPc-NH_2/CNT with a commercially available Cu microparticle catalyst known to support CO reduction current density up to several hundred mA cm^{-2}.[30] Indeed, the Cu catalyst delivered a CO reduction partial current density of 140 mA cm^{-2} at a total current density of 200 mA cm^{-2} (Figure 3a). In contrast, under the same operating conditions, the CoPc-NH_2/CNT catalyst only gave a j_{MeOH} of 17.6 mA cm^{-2} (Figure 2i). This result suggested that our flow cell was well-constructed and operated, and that the difference might be between the metal and molecular catalysts. Through quantifying the numbers of electrochemically active sites using cyclic voltammetry (Figures S4, S6, S7), we determined that the CoPc-NH_2/CNT catalyst has approximately one-third the number of active sites as Cu at the given catalyst loadings (Figure 3b, 0.4 mg cm^{-2} for CoPc-NH_2/CNT and 1.0 mg cm^{-2} for Cu). At a total current density of 100 mA cm^{-2}, the CoPc-NH_2/CNT catalyst showed a higher turnover frequency (TOF, 6.3 s^{-1}) than that of the Cu catalyst (4.3 s^{-1}). However, the TOF of Cu increased to 9.5 s^{-1} at 200 mA cm^{-2}, while that of CoPc-NH_2/CNT slightly decreased.

Since the CoPc-NH_2/CNT catalyst, at the mass loading of 0.4 mg cm^{-2}, appeared to have fewer and less active sites than Cu (at 1.0 mg cm^{-2}) for CO reduction, we thought to improve the reaction rate by increasing the catalyst loading on the electrode. However, even with an increased CoPc-NH_2/CNT mass loading of 1.2 mg cm^{-2}, j_{MeOH} still remained limited to around 20 mA cm^{-2} at total current densities up to 250 mA cm^{-2} (Figure S8). This led us to believe that the additional CoPc-NH_2 sites from the increased catalyst loading primarily contributed to H_2 evolution rather than CO reduction (Figure S9). We suspected that these sites were buried in the electrolyte so that CO was not delivered sufficiently due to its low solubility. To test this hypothesis, we utilized scanning electron microscopy (SEM) and energy dispersive X-ray spectroscopy (EDX) to map the distribution of K^+ ions in the cross-section of the electrode after electrolysis, which will reflect the situation of electrolyte penetration into the catalyst layer.[31] Strong K signals were detected in the CoPc-NH_2/CNT electrode, indicating severe electrolyte penetration into the catalyst layer (Figure 3d and Figures S10, S11). In contrast, the Cu catalyst layer showed a much lower affinity to the electrolyte (Figure 3c). This notable difference between the two catalysts is likely associated with their different density, porosity, and surface hydrophilicity. The polar bonds in the CoPc-NH_2 molecular structure and the porous structure of the CNT support network render the catalyst layer prone to electrolyte occupation, making the active sites difficult to access by the insoluble CO reactant. For thicker CoPc-NH_2/CNT electrodes, the entire catalyst layer was embedded in the electrolyte (Figures S12 and S13). In this scenario, only the catalytic sites close to the gas phase can perform CO reduction; the deeper sites close to the electrolyte are deprived of CO and thus mainly catalyze H_2 evolution. Based on this comparison, we formulated two ideas for improving the CO reduction rate of the molecular catalyst. One is to develop different and more effective catalyst/electrode modifications than those used for Cu. The other is to take advantage of the high solubility of CO_2 and provide CO *in situ*.

CO_2 Reduction Performance. To test the second idea for addressing this challenge, we considered using CO_2 as the reactant for methanol production. CO_2 has a faster diffusion rate in the electrolyte than CO due to its higher solubility and can sustain a higher reaction rate even when the catalyst layer is partially flooded.[32] Effective CO_2 reduction can generate CO *in situ* near the catalytic sites to support further reduction into methanol. After optimizing the structural and operational parameters (Figure S14), we evaluated the CO_2 reduction performance under constant current conditions (Table S4). Up to a current density of 100 mA cm^{-2}, CO was the major product (Figure 4a), showing effective CO_2-to-CO conversion over the molecular catalyst at relatively low overpotentials.[33] As the current density was increased, methanol formation was accelerated and FE_{MeOH} increased continuously up to 43% at a total current density of 300 mA cm^{-2}, reaching a j_{MeOH} of 129 mA cm^{-2} (Figure 4a). Meanwhile, FE_{CO} decreased with increasing total current density, indicating the consumption of CO as an intermediate in the CO_2-to-methanol conversion process. Note that the selectivity for methanol is enhanced compared to the highest FE_{MeOH} of 32% obtained in the H-cell, possibly due to accelerated CO_2-to-CO conversion in the GDE, and the methanol production rate is approximately 12 times improved in the flow cell (Figure 4b).[12] This production rate stands as the highest reported for the electroreduction of CO_2/CO into methanol catalyzed by molecular catalysts (Table S5).

In contrast to the limited increase in j_{MeOH} observed for CO reduction, this outcome underscores that *in situ* generated CO from CO_2 reduction is more effective in providing a sufficient amount of local CO for producing methanol than direct CO reduction with a CO gas supply, which is supported by our theoretical modeling of CO fluxes in both cases (Figure S15). This effectiveness is a direct consequence of the electrolyte-philic microenvironment of the molecular catalyst: high-rate

https://doi.org/10.1021/jacs.4c05961
J. Am. Chem. Soc. 2024, 146, 16348−16354

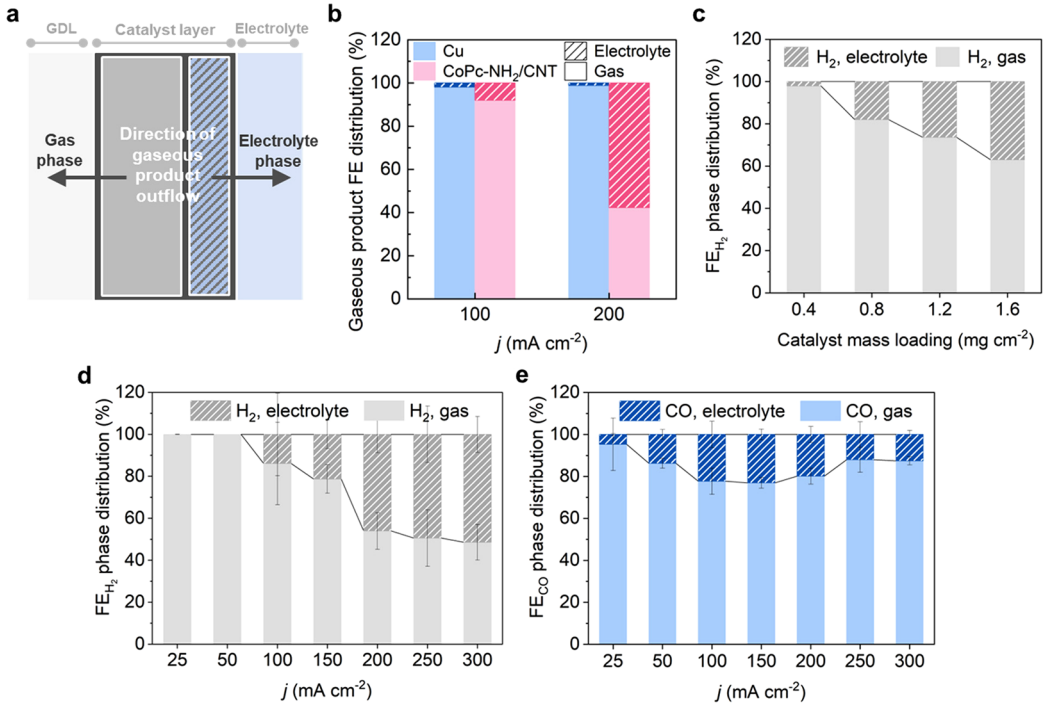

Figure 5. Gaseous product separation into different phases. (a) Schematic for the separation of gaseous products generated in the catalyst layer into the gas phase through the gas diffusion layer or into the electrolyte phase. (b) Comparison of the normalized phase distribution of gaseous products between Cu microparticle and CoPc-NH_2/CNT catalysts for CO reduction. (c) Normalized phase distribution of H_2 with different mass loadings of CoPc-NH_2/CNT for CO reduction at a total current density of 50 mA cm^{-2}. Normalized phase distributions of (d) H_2 and (e) CO for CO_2 reduction catalyzed by CoPc-NH_2/CNT at different total current densities.

methanol production from CO_2 reduction supports our conjecture that CO accessibility by the catalytic sites is the main reason for the limited current density in CO reduction.[18] Moreover, this *in situ* CO generation strategy enables more catalytic sites to be utilized for methanol production. Unlike direct CO reduction, both the selectivity and reaction rate in CO_2 reduction to methanol exhibited improvement with a thicker catalyst layer, up to a mass loading of 1.2 mg cm^{-2} (Figure S14b). We would like to emphasize that using CO_2 as the reactant has at least two advantages: 1) it increases the methanol production current density to a record-high level, and 2) it directly consumes CO_2 as opposed to CO reduction which needs to be coupled with another reactor reducing CO_2 to CO. Stability of CO_2 reduction catalyzed by CoPc-NH_2/CNT was tested at the constant current density of 150 mA cm^{-2} for 5 h. Stable performance with no significant decrease in methanol FE was achieved (Figure S16). Worse stability was observed at higher current densities likely due to GDE flooding. More approaches to exclude the flooding effect under high current/potential conditions are needed in future work.

Phase Separation of Gaseous Products. During the electrolysis using the CoPc-NH_2/CNT catalyst, we discovered that a portion of the gaseous products was detected in the catholyte container, even when the feed gas and catholyte flow rates were adjusted (Figures S17a, b). This observation implies that not all gaseous products diffuse out to the gas phase through the gas diffusion layer, but some of them are instead discharged into the electrolyte phase (Figure 5a). Under 100 mA cm^{-2} of CO reduction, 8.1% (all the phase distribution percentages reported in this work are based on FE) of the gaseous products were discharged into the electrolyte phase, which increased substantially to 58% at a total current density of 200 mA cm^{-2} (Figure 5b). This phenomenon is closely linked to the electrolyte-philic property of the CoPc-NH_2/CNT catalyst. On the contrary, the Cu catalyst discharged 99% of the gaseous products through the gas diffusion layer into the gas phase even at 200 mA cm^{-2}. As the thickness of the CoPc-NH_2/CNT catalyst layer was increased from 0.4 to 1.6 mg cm^{-2}, a progressively larger portion of H_2 was discharged into the electrolyte phase (Figure 5c). The thicker the catalyst layer, the more active sites are immersed in the electrolyte, hindering the diffusion of H_2 into the gas phase.

Interestingly, the phase distributions of the two gaseous products in CO_2 reduction catalyzed by CoPc-NH_2/CNT showed a notable discrepancy. In the case of H_2, the portion discharged into the electrolyte phase steadily increased from an undetectable level to 51% at a total current density of 300 mA cm^{-2} (Figure 5d), which is in line with the observations in CO reduction (Figure 5b). However, for CO, as the total current density was increased, the electrolyte phase portion rose, plateaued to 23% at 150 mA cm^{-2}, and then gradually decreased to 13% at 300 mA cm^{-2} (Figure 5e). It is worth emphasizing that 150 mA cm^{-2} is the lowest total current density where a considerable j_{MeOH} is observed (Figure 4a). This decreasing tendency of CO effluence through the electrolyte phase suggests that CO generated deep inside the catalyst layer is likely consumed to form methanol. These findings collectively support that the high methanol production rate from CO_2 reduction originates from the effective utilization of locally generated CO within the electrolyte-occupied molecular catalyst region.

https://doi.org/10.1021/jacs.4c05961
J. Am. Chem. Soc. 2024, 146, 16348−16354

CONCLUSION

Our exploration of the CoPc-NH_2/CNT molecular catalyst in a flow cell for electrochemical CO reduction to methanol has revealed a limitation linked to the depletion of the reactant within the electrolyte-philic catalyst layer. Shifting to CO_2 as the reactant enables the utilization of more catalytic sites through locally generated CO, resulting in a methanol partial current density of 130 mA cm^{-2}. These findings underscore the unique attributes of molecular catalysts distinct from prevalently studied metal particle-based ones and demonstrate the importance of microenvironment management near the active sites in achieving high current density for practical operation.

ASSOCIATED CONTENT

Supporting Information

The Supporting Information is available free of charge at https://pubs.acs.org/doi/10.1021/jacs.4c05961.

Experimental and modeling methods, structural characterization of CoPc-NH_2/CNT, and additional electrochemical reaction results for CoPc-NH_2/CNT and Cu (PDF)

AUTHOR INFORMATION

Corresponding Author

Hailiang Wang − *Department of Chemistry, Yale University, New Haven, Connecticut 06520, United States; Energy Sciences Institute, Yale University, West Haven, Connecticut 06516, United States;* orcid.org/0000-0003-4409-2034; Email: hailiang.wang@yale.edu

Authors

Seonjeong Cheon − *Department of Chemistry, Yale University, New Haven, Connecticut 06520, United States; Energy Sciences Institute, Yale University, West Haven, Connecticut 06516, United States*

Jing Li − *Department of Chemistry, Yale University, New Haven, Connecticut 06520, United States; Energy Sciences Institute, Yale University, West Haven, Connecticut 06516, United States;* orcid.org/0000-0001-7538-246X

Complete contact information is available at: https://pubs.acs.org/10.1021/jacs.4c05961

Notes

The authors declare no competing financial interest.

ACKNOWLEDGMENTS

This work was supported by the Yale Center for Natural Carbon Capture and the US National Science Foundation (CHE-2154724).

REFERENCES

(1) Gawel, A.; Jaster, T.; Siegmund, D.; Holzmann, J.; Lohmann, H.; Klemm, E.; Apfel, U. P. Electrochemical CO2 Reduction - The Macroscopic World of Electrode Design, Reactor Concepts & Economic Aspects. *iScience.* **2022**, *25*, No. 104011.

(2) Artz, J.; Müller, T. E.; Thenert, K.; Kleinekorte, J.; Meys, R.; Sternberg, A.; Bardow, A.; Leitner, W. Sustainable Conversion of Carbon Dioxide: An Integrated Review of Catalysis and Life Cycle Assessment. *Chem. Rev.* **2018**, *118*, 434−504.

(3) Kibria Nabil, S.; McCoy, S.; Kibria, M. G. Comparative Life Cycle Assessment of Electrochemical Upgrading of CO2 to Fuels and Feedstocks. *Green Chem.* **2021**, *23* (2), 867−880.

(4) Li, L.; Li, X.; Sun, Y.; Xie, Y. Rational Design of Electrocatalytic Carbon Dioxide Reduction for a Zero-Carbon Network. *Chemical Society Reviews.* **2022**, *51*, 1234−1252.

(5) Navarro-Jaén, S.; Virginie, M.; Bonin, J.; Robert, M.; Wojcieszak, R.; Khodakov, A. Y. Highlights and Challenges in the Selective Reduction of Carbon Dioxide to Methanol. *Nature Reviews Chemistry.* **2021**, *5*, 564−579.

(6) Sollai, S.; Porcu, A.; Tola, V.; Ferrara, F.; Pettinau, A. Renewable Methanol Production from Green Hydrogen and Captured CO2: A Techno-Economic Assessment. *J. CO2 Util.* **2023**, *68*, No. 102345.

(7) Zhang, J.; Yu, P.; Peng, C.; Lv, X.; Liu, Z.; Cheng, T.; Zheng, G. Efficient CO Electroreduction to Methanol by CuRh Alloys with Isolated Rh Sites. *ACS Catal.* **2023**, *13*, 7170−7177.

(8) Zhu, N.; Zhang, X.; Chen, N.; Zhu, J.; Zheng, X.; Chen, Z.; Sheng, T.; Wu, Z.; Xiong, Y. Integration of MnO 2 Nanosheets with Pd Nanoparticles for Efficient CO 2 Electroreduction to Methanol in Membrane Electrode Assembly Electrolyzers. *J. Am. Chem. Soc.* **2023**, DOI: 10.1021/jacs.3c09307.

(9) Kong, S.; Lv, X.; Wang, X.; Liu, Z.; Li, Z.; Jia, B.; Sun, D.; Yang, C.; Liu, L.; Guan, A.; et al. Delocalization State-Induced Selective Bond Breaking for Efficient Methanol Electrosynthesis from CO2. *Nat. Catal.* **2023**, *6* (1), 6−15.

(10) Hu, M. K.; Wang, N.; Ma, D. D.; Zhu, Q. L. Surveying the Electrocatalytic CO2-to-CO Activity of Heterogenized Metallomacrocycles via Accurate Clipping at the Molecular Level. *Nano Res.* **2022**, *15* (12), 10070−10077.

(11) Xu, H.; Cai, H.; Cui, L.; Yu, L.; Gao, R.; Shi, C. Molecular Modulating of Cobalt Phthalocyanines on Amino-Functionalized Carbon Nanotubes for Enhanced Electrocatalytic CO2 Conversion. *Nano Res.* **2023**, *16* (3), 3649−3657.

(12) Wu, Y.; Jiang, Z.; Lu, X.; Liang, Y.; Wang, H. Domino Electroreduction of CO2 to Methanol on a Molecular Catalyst. *Nature* **2019**, *575* (7784), 639−642.

(13) Rooney, C. L.; Lyons, M.; Wu, Y.; Hu, G.; Wang, M.; Choi, C.; Gao, Y.; Chang, C. W.; Brudvig, G. W.; Feng, Z.; et al. Active Sites of Cobalt Phthalocyanine in Electrocatalytic CO2 Reduction to Methanol. *Angew. Chemie - Int. Ed.* **2024**, *63* (2), No. e202310623.

(14) Wu, Y.; Liang, Y.; Wang, H. Heterogeneous Molecular Catalysts of Metal Phthalocyanines for Electrochemical CO 2 Reduction Reactions. *Acc. Chem. Res.* **2021**, *54* (16), 3149−3159.

(15) Li, J.; Shang, B.; Gao, Y.; Cheon, S.; Rooney, C. L.; Wang, H. Mechanism-Guided Realization of Selective Carbon Monoxide Electroreduction to Methanol. *Nat. Synth.* **2023**, *2*, 1194.

(16) Ripatti, D. S.; Veltman, T. R.; Kanan, M. W. Carbon Monoxide Gas Diffusion Electrolysis That Produces Concentrated C2 Products with High Single-Pass Conversion. *Joule* **2019**, *3*, 240−256.

(17) Rabiee, H.; Ge, L.; Zhang, X.; Hu, S.; Li, M.; Yuan, Z. Gas Diffusion Electrodes (GDEs) for Electrochemical Reduction of Carbon Dioxide, Carbon Monoxide, and Dinitrogen to Value-Added Products: A Review. *Energy Environ. Sci.* **2021**, *14* (4), 1959.

(18) Nesbitt, N. T.; Burdyny, T.; Simonson, H.; Salvatore, D.; Bohra, D.; Kas, R.; Smith, W. A. Liquid−Solid Boundaries Dominate Activity of CO 2 Reduction on Gas-Diffusion Electrodes. *ACS Catal.* **2020**, *10* (23), 14093−14106.

(19) Burdyny, T.; Smith, W. A. CO 2 Reduction on Gas-Diffusion Electrodes and Why Catalytic Performance Must Be Assessed at Commercially-Relevant Conditions. *Energy Environ. Sci.* **2019**, *12* (5), 1442−1453.

(20) Su, J.; Musgrave, C. B.; Song, Y.; Huang, L.; Liu, Y.; Li, G.; Xin, Y.; Xiong, P.; Li, M. M.-J.; Wu, H.; et al. Strain Enhances the Activity of Molecular Electrocatalysts via Carbon Nanotube Supports. *Nat. Catal.* **2023**, *6*, 818−828.

(21) Ren, X.; Zhao, J.; Li, X.; Shao, J.; Pan, B.; Salamé, A.; Boutin, E.; Groizard, T.; Wang, S.; Ding, J.; et al. In-Situ Spectroscopic Probe of the Intrinsic Structure Feature of Single-Atom Center in Electrochemical CO/CO2 Reduction to Methanol. *Nat. Commun.* **2023**, *14* (1), 3401.

(22) Ding, J.; Wei, Z.; Li, F.; Zhang, J.; Zhang, Q.; Zhou, J.; Wang, W.; Liu, Y.; Zhang, Z.; Su, X.; et al. Atomic High-Spin Cobalt(II)

Center for Highly Selective Electrochemical CO Reduction to CH3OH. *Nat. Commun.* **2023**, *14* (1), 6550.
(23) Yao, L.; Rivera-Cruz, K. E.; Zimmerman, P. M.; Singh, N.; McCrory, C. C. L. Electrochemical CO 2 Reduction to Methanol by Cobalt Phthalocyanine: Quantifying CO 2 and CO Binding Strengths and Their Influence on Methanol Production. *ACS Catal.* **2024**, *14*, 366−372.
(24) Wen, G.; Ren, B.; Wang, X.; Luo, D.; Dou, H.; Zheng, Y.; Gao, R.; Gostick, J.; Yu, A.; Chen, Z. Continuous CO2 Electrolysis Using a CO2 Exsolution-Induced Flow Cell. *Nat. Energy* **2022**, *7* (10), 978−988.
(25) Xie, Y.; Ou, P.; Wang, X.; Xu, Z.; Li, Y. C.; Wang, Z.; Huang, J. E.; Wicks, J.; McCallum, C.; Wang, N.; et al. High Carbon Utilization in CO2 Reduction to Multi-Carbon Products in Acidic Media. *Nat. Catal.* **2022**, *5* (6), 564−570.
(26) Grigioni, I.; Sagar, L. K.; Li, Y. C.; Lee, G.; Yan, Y.; Bertens, K.; Miao, R. K.; Wang, X.; Abed, J.; Won, D. H.; et al. CO2 Electroreduction to Formate at a Partial Current Density of 930 MA Cm-2with InP Colloidal Quantum Dot Derived Catalysts. *ACS Energy Lett.* **2021**, *6* (1), 79−84.
(27) Ge, L.; Rabiee, H.; Li, M.; Subramanian, S.; Zheng, Y.; Lee, J. H.; Burdyny, T.; Wang, H. Electrochemical CO2 Reduction in Membrane-Electrode Assemblies. *Chem.* **2022**, *8* (3), 663−692.
(28) Kim, C.; Bui, J. C.; Luo, X.; Cooper, J. K.; Kusoglu, A.; Weber, A. Z.; Bell, A. T. Tailored Catalyst Microenvironments for CO2 Electroreduction to Multicarbon Products on Copper Using Bilayer Ionomer Coatings. *Nat. Energy* **2021**, *6* (11), 1026−1034.
(29) García de Arquer, F. P.; Dinh, C.-T.; Ozden, A.; Wicks, J.; McCallum, C.; Kirmani, A. R.; Nam, D.-H.; Gabardo, C.; Seifitokaldani, A.; Wang, X.; et al. CO 2 Electrolysis to Multicarbon Products at Activities Greater than 1 A Cm − 2. *Science (80-.).* **2020**, *367* (6478), 661−666.
(30) Jouny, M.; Luc, W.; Jiao, F. High-Rate Electroreduction of Carbon Monoxide to Multi-Carbon Products. *Nat. Catal.* **2018**, *1* (10), 748−755.
(31) Inoue, A.; Harada, T.; Nakanishi, S.; Kamiya, K. Ultra-High-Rate CO 2 Reduction Reactions to Multicarbon Products with a Current Density of 1.7 A Cm − 2 in Neutral Electrolytes. *EES Catal.* **2023**, *1* (1), 9−16.
(32) Zhang, T.; Li, Z.; Lyu, X.; Raj, J.; Zhang, G.; Kim, H.; Wang, X.; Chae, S.; Lemen, L.; Shanov, V. N.; et al. The Conventional Gas Diffusion Electrode May Not Be Resistant to Flooding during CO 2 /CO Reduction. *J. Electrochem. Soc.* **2022**, *169* (10), No. 104506.
(33) Corbin, N.; Zeng, J.; Williams, K.; Manthiram, K. Heterogeneous Molecular Catalysts for Electrocatalytic CO2 Reduction. *Nano Res.* **2019**, *12* (9), 2093−2125.

https://doi.org/10.1021/jacs.4c05961
J. Am. Chem. Soc. 2024, 146, 16348−16354